Sobolev, S. V., Babeyko, A. Y., Wang, R., Galas, R., Rothacher, M., Stein, D., Schröter, J., Lauterjung, J., Subarya, C. (2006): Towards Real-Time Tsunami Amplitude Prediction. - Eos, Transactions, American Geophysical Union, 87, 37, 374, 378.

http://www.agu.org/journals/eo/eo0637/2006EO370003.pdf#anchor

GPS-Shield: reliable prediction of tsunami amplitude within less than 10 minutes of an earthquake

Stephan V. Sobolev, Andrey Y. Babeyko, Rongjiang Wang, Roman Galas, Markus Rothacher, Dmitry V. Sein, Jens Schröter, Jorn Lauterjung and Cecep Subarya

The catastrophic 2004 Indian Ocean tsunami triggered a number of initiatives aimed at establishing modern and robust tsunami early warning systems. The greatest challenge of the GITEWS (German Indonesian Tsunami Early Warning System), led by the National Center of Geosciences (GeoForschungsZentrum) in Potsdam, Germany, is to provide early tsunami warning for the Indian-Ocean coast of Indonesia where tsunami are expected to arrive 20-30 minutes after an earthquake. In this communication, we show that reliable prediction of tsunami wave heights at the Sumatran coast cannot be provided using traditional, earthquake-magnitude-based methods. Instead, we suggest a novel real-time warning technique based on special types of near-field GPS arrays ('GPS Shield') that are appropriate for Sumatra and elsewhere around the globe.

Possible future tsunamis in Sumatra

Another great earthquake near Sumatra may occur south of the 2005 March rupture zone [Pollitz et al., 2006] and may well be similar to the $M_w \approx 8$-9 earthquakes that occurred in this region in 1797 and 1833 [Sieh et al., 2004]. The excited tsunami may be especially dangerous for the nearby city of Padang, which has more than 750,000 inhabitants.

We computed the propagation of tsunami waves (see Appendix for technical details) for two possible rupture models of this future earthquake. Both models have the same seismic moment (M_w=9), rupture geometry and average coseismic slip of 8.5 m (the latter is consistent with the assumption of complete locking of the seismogenic zone since 1833). The only difference between these two models is the slip distribution: model A has a slip maximum in the shallow part of the rupture, while in model B the maximum slip is in the deeper part. We solved numerically nonlinear shallow-water equations in spherical coordinates using an explicit-in-time finite element integration scheme on an unstructured grid (grid spacing changes from 15 km in the deep ocean to 150 m close to the coast) and with wetting-drying boundary condition at the coast. In our model, we employed 1 arc minute GEBCO bathymetry data supplemented by recently-obtained detailed data for the Sumatra region.

Calculated tsunami wave fields are remarkably different for the two considered rupture scenarios. Model A generates maximum uplift west of the Mentawai islands and, due to the screening effect of the islands, a relatively small tsunami is expected near the city of Padang (Figure 1). In contrast, rupture model B generates very high tsunami waves at Padang, but smaller waves traveling into the open ocean. Resulting maximum wave heights at Padang induced by models A and B differ by a factor of more than 5 (Figure 1, inset).

We emphasize that the two rupture scenarios which generate such different tsunamis at Padang have the *same seismic moment (magnitude)* and may well be characterized by the *same hypocenter location.* Therefore, in order to distinguish between models A and B it is not enough to know these parameters, but it is also necessary to resolve higher-order features of slip distribution on the fault. An indication of how to accomplish this comes from recent advances in the use of GPS techniques in the study of coseismic displacements caused by the great Sumatran earthquake of 2004 [Vigny et al., 2005; Subarya et al., 2006]. However, while available GPS data are likely sufficient to allow estimation of the magnitude of the 2004 event [Blewitt et al., 2006], various inversions of the GPS data give different results for the slip distribution on the faults. This suggests that these data do not provide enough depth resolution.

We propose implementing specially-aligned arrays of 2-3 high-rate, real-time GPS stations located close to the source (in the case of Sumatra, on the Mentawai islands) that will provide the much-improved slip resolution that is especially important for early tsunami warning for Sumatra. Such arrays will exploit large displacements and their trench-perpendicular gradients in the near-field. Note that the Caltech/LIPI SuGAR GPS network already has continuous GPS sites in some of the appropriate places, but unfortunately none of those sites are yet equipped to allow for real-time applications.

Concept of 'GPS Shield' for Sumatra

Key elements of the "GPS Shield" concept for Sumatra are arrays of several real-time high-rate (1-10 Hz) GPS stations located on the islands west of Sumatra and at the Sumatran coast (Figure 2). Stations on the islands are closely spaced (10-20 km) and aligned perpendicular to the trench, i.e., parallel to the expected gradient of surface coseismic displacement. The arrays measure surface displacements using instantaneous GPS positioning techniques [Bock et al., 2000] that, for single-epoch 1-Hz displacement measurements, achieve an accuracy of better than several centimeters for absolute displacements and a few centimeters for relative displacements between the closely-spaced stations. The GPS-Shield arrays are set along the trench with a spacing of 100-200 km, a spacing that is appropriate to resolve major trench-parallel slip heterogeneity. In the case where there are no islands between the trench and Sumatra, we suggest the use of ocean buoys equipped with GPS devices and bottom pressure sensors.

To examine the functionality of the proposed system, we simulated the entire rupture process using a 3D numerical model. Synthetic seismograms for the scenario earthquake are calculated using the deterministic Green's function method based on the IASPEI91 layered-Earth model. In this simulation, the rupture starts in the deep part of the seismogenic zone east of Siberut Island (star in Figure 2) and propagates up-dip and southwards in a trench-parallel direction with a velocity of 2.5 km/s. Synthetic displacement seismograms at the two GPS stations on Siberut island and one station in Padang are shown in the upper inset of Figure 2.

In this model, the first seismic signal arrives at Siberut and Padang stations less than 20 s after the rupture starts; this arrival can be used to switch the observational network into a high sampling-rate mode. After less than 6-7 minutes, static displacements are fully established at the stations closest to the epicenter (Figure 2, upper inset), and rupture parameters and, hence, initial tsunami wave form can be resolved by the inversion procedure (Figure 2, lower inset and Appendix). After 6-7 minutes, the tsunami wave has already passed the tide gauge at Siberut Island, allowing verification of the estimated rupture parameters. Therefore, we expect that the qualified tsunami warning for the region of Padang can be issued less than 6-7 minutes after the rupture begins. At that time it will be possible to predict the tsunami wave heights very well and thus to distinguish between catastrophic and less dangerous scenarios. This leaves more than 18 minutes before the tsunami hits the coast at Padang.

In addition, it is useful to complement some of the GPS stations with broad-band seismometers and strong-motion recorders (white circles in Figure 2). It was recently demonstrated [Banerjee et al., 2005] that slip inversions from GPS data are very sensitive to assumed fault geometry, especially when relying on the near-field data. Therefore, precise mapping of the seismogenic-zone geometry, which can be accomplished only with long-term observations using the broad-band seismometers, is essential for the success of the GPS-Shield concept.

In the inversion procedure, we employ distributed slip parameterization [Geist & Dmowska, 1999] to characterize rupture. For given rupture parameters (models A and B), horizontal and vertical displacements at the surface are calculated using an elastic dislocation model in a layered half-space [Wang et al, 2006]. Displacements at GPS-array stations, altered by random noise to mimic real-time GPS accuracy, are then inverted for rupture parameters using a non-linear simplex method. Grey and black curves in the lower inset in Figure 2 show results of 1000 such inversions. To be conservative, we assumed modest measurement accuracies of +-10 cm and +-5 cm for absolute vertical and horizontal displacements, as well as +-3 cm and +-1 cm for relative vertical and horizontal displacements between the stations.

Global implication

Our analysis (Sobolev et al., submitted) shows that GPS-Shield arrays can resolve tsunami-controlling rupture parameters very well, provided they are placed above the rupture zone (Figure 2, lower inset). By moving the array landwards, the resolution decreases, but it remains fair until the array is moved away some 50-100 km from the surface projection of the rupture zone. Arrays located still further from the trench strongly decrease the resolution and can resolve neither average slip on the fault, nor the depth of the slip maximum, but they still allow the estimation, with high accuracy, of the seismic moment of a giant earthquake, even at a distance of 500 km from the trench.

These results suggest that GPS-Shield arrays can be efficiently used at most of tsunamigenic active margins. The best results in predicting tsunami waves within less than 10 min of an earthquake can be obtained where the land is located closer than 100 km to the seismogenic zone (solid curves in Figure 3). If the land is located at larger distances, but still closer than 500 km from the trench (dashed curves in Figure 3), the GPS-Shield arrays can be used at least for fast and precise estimation of the seismic moment of large earthquakes. It is also important to mention that the global GPS-Shield arrays will in fact serve two important purposes. In addition to their tsunami-warning function described above, the arrays will also allow long-term deformation monitoring in most convergent plate boundaries. This function will provide important data for constraining global geodynamics and, in particular, the processes that lead to large megathrust earthquakes.

Acknowledgements

This is publication no. 6 of the GITEWS project (German Indian ocean Tsunami Early Warning System) funded by the German Federal Ministry for Education and Research (BMBF), Grant 03TSU01. Ernst Flüh provided unpublished bathymetry data. Discussion and comments by Roland Bürgmann were very helpful for improving the manuscript. We are also grateful to Ron Hackney and Kevin Fleming for useful comments and editorial help and to the members of the GITEWS team for stimulating discussions.

References

Banerjee, P. , Pollitz, F. F. & R. Burgmann, The size and duration of the Sumatra-Andaman earthquake from far-field static offsets. *Science* **308**, 1769-1772 (2005).

Bock, Y. et al., Instantaneous geodetic positioning at medium distances with the Global Positioning System. *J. Geophys. Res.* **105**, 28223–28254 (2000).

Blewitt, G. et al., Rapid determination of earthquake magnitude using GPS for tsunami warning systems. *Geophys. Res. Lett.*, **33**, L11309 (2006).

Geist, E. L. & Dmowska, R., Local tsunamis and distributed slip at the source. *Pure Appl. Geophys.* **154,** 485–512 (1999).

Pollitz, F. F.et al., Stress changes along the Sunda trench following the 26 December 2004 Sumatra-Andaman and 28 March 2005 Nias earthquakes. *Geophys. Res. Lett.* **33**, L06309, doi:10.1029/2005GL024558 (2006).

Sieh, K. et al., The giant subduction earthquakes of 1797 and 1833, West Sumatra: Characteristic couplets, uncharacteristic slip. *Eos Trans. AGU* **85(47)** Fall Meet. Suppl., Abstract T12B-04 (2004).

Subarya, C. et al., Plate-boundary deformation associated with the great Sumatra–Andaman earthquake. *Nature* **440**, doi: 10.1038/nature04522 (2006).

Sobolev et al., Concept for fast and reliable tsunami early warning using "GPS-Shield" arrays. *JGR, Submitted*

Vigny, C.et al. Insight into the 2004 Sumatra-Andaman earthquake from GPS measurements in southeast Asia., *Nature* **436**, 201-206 (2005).

Wang, R., Lorenzo-Martín, F. & Roth, F. PSGRN/PSCMP - a new code for calculating co- and post-seismic deformation, geoid and gravity changes based on the viscoelastic-gravitational dislocation theory. *Computers and Geosciences* **32**, 527-541 (2006).

Figure captions

Figure 1. Maximum tsunami heights for rupture models with shallow (A) and deep (B) slip maximum. Inset shows computed tsunami run-ups close to the city of Padang.

Figure 2. The 'GPS-shield' for Sumatra. The conceptual distribution of observational instruments is shown. Red circles are real-time GPS stations (those with white rings are also equipped with broad-band seismometers and accelerometers). Red diamonds are GPS-equipped buoys. The upper inset shows the synthetic horizontal and vertical surface

displacements at two GPS stations on Siberut island and one station in Padang that are induced by a M_w=9 earthquake whose epicenter is indicated by star and rupture area marked by the dashed line. Lower inset - reconstructions of tsunamogenic sea-bottom displacements from inversion of synthetic observations at the three-station GPS array (triangles). Note almost perfect reconstructions (black lines) of the input signals (colored lines) and robust discrimination between less- and more-dangerous rupture scenarios (A) and (B) (see Appendix for inversion details).

Figure 3. Global application of the GPS-Shield concept. Solid lines show subduction zones where the land is located closer than 100 km to the seismogenic zone, i.e. where the GPS-Shield arrays can resolve major features of slip distribution on the fault within less than 10 minutes of an earthquake. Dashed lines are the zones where the GPS-Shield arrays can at least resolve the seismic moment of the closest large earthquakes, also within less than 10 minutes of an earthquake.

Author information

Stephan Sobolev, GeoForschungsZentrum Potsdam, Germany and Institute of Physics of the Earth, Moscow, E-mail: stephan@gfz-potsdam.de; Andrey Babeyko, Rongjiang Wang, Roman Galas, Markus Rothacher and Jorn Lauterjung, GeoForschungsZentrum Potsdam, Germany; _Dmitry Sein and Jens Schröter, Alfred Wegener Institute, Bremerhaven, Germany; Cecep Subarya, BAKOSURTANAL, Jakarta, Indonesia

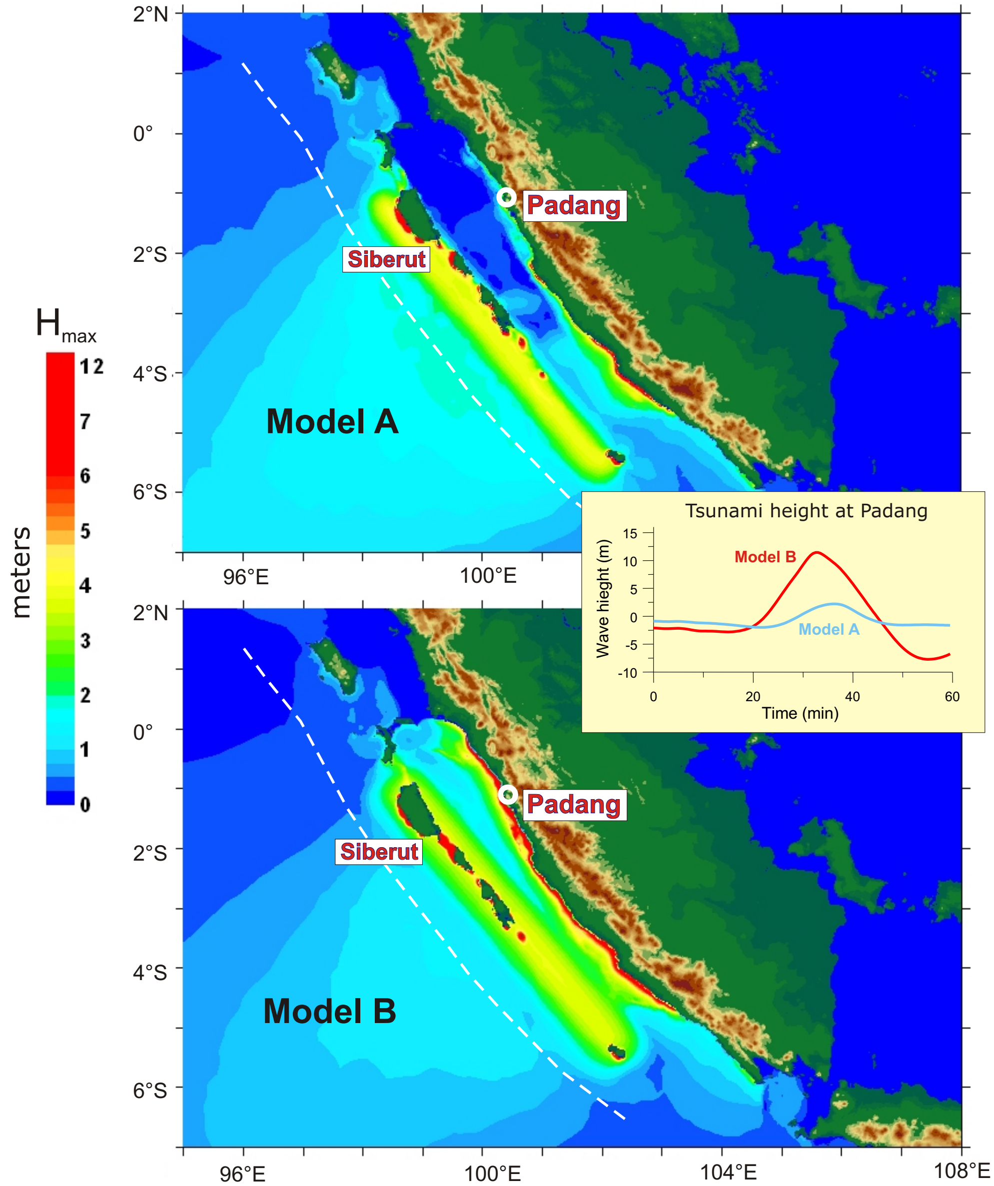

GPS-Shield, Fig. 1

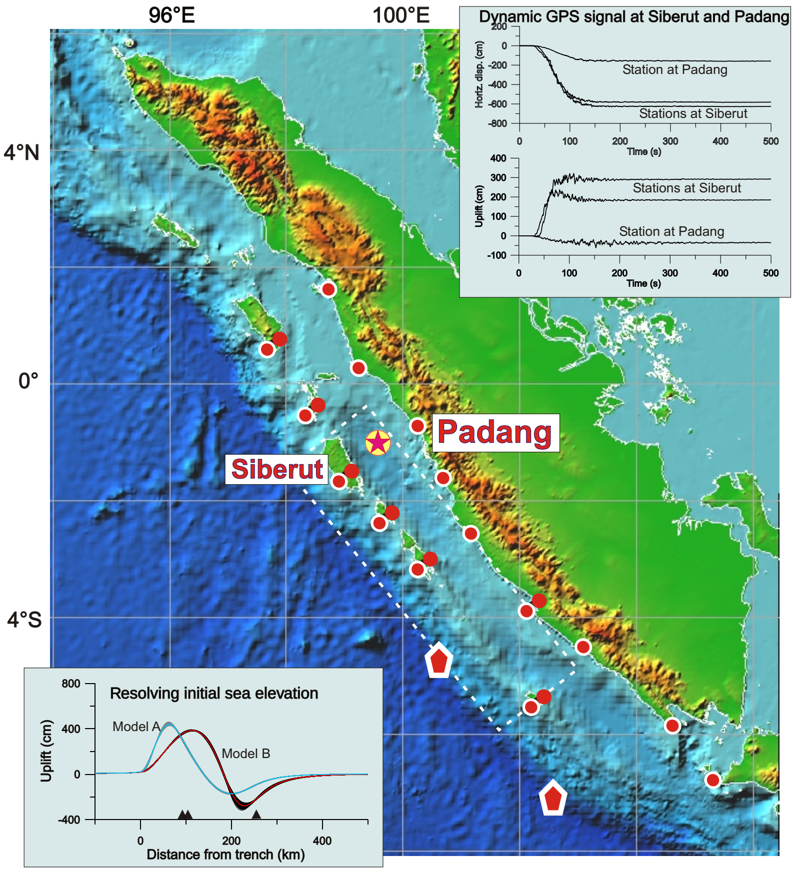

GPS-Shield, Fig. 2

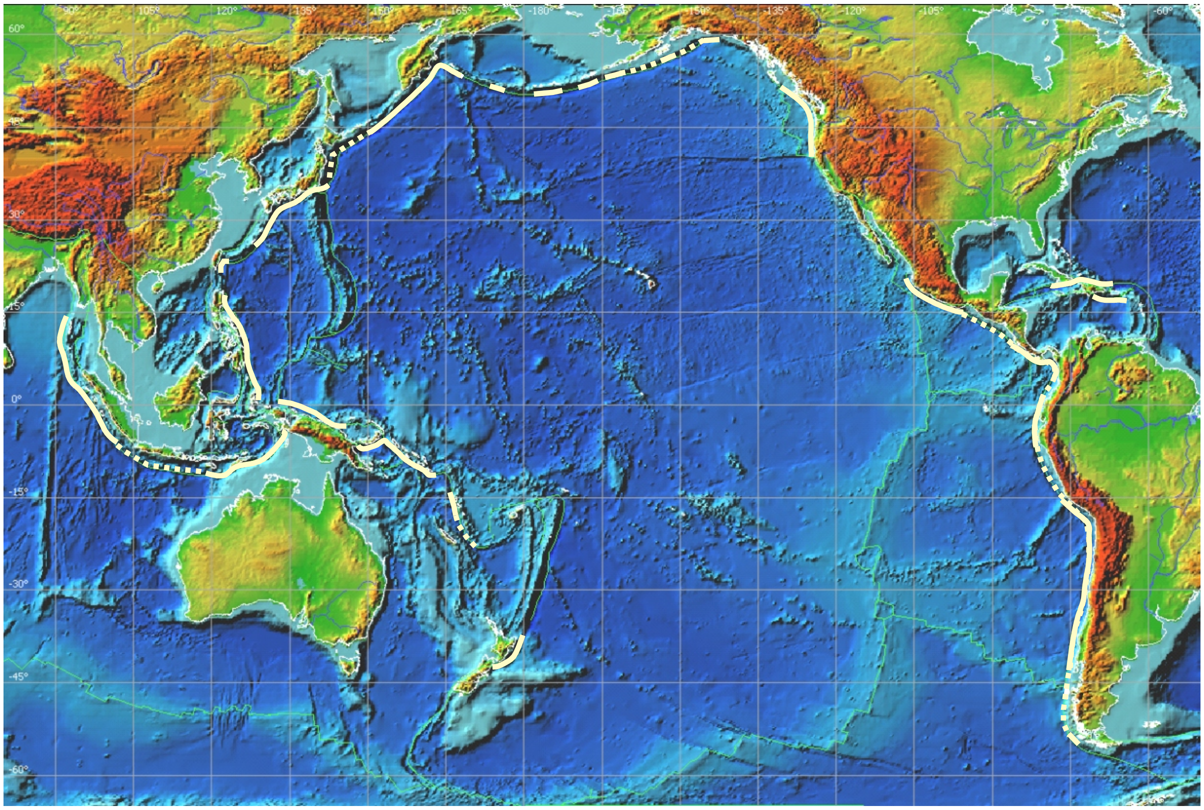

GPS-Shield, Fig. 3